ANISOTROPIC DUCTILE RUPTURE

A. A. Benzerga*, J. Besson*, R. Batisse†, A. Pineau*

The aim of this article is to study the effect of inclusion shape on ductile fracture anisotropy of a C–Mn steel containing MnS inclusions. For this purpose, a Gurson–like model incorporating void shape effect has been implemented in a finite element software.The model is tested for varying stress triaxialities and initial void aspect ratios. It is then applied to discuss the differences in strains to failure measured on axisymmetric notched bars tested along different directions. In order to determine the appropriate initial parameters, namely the void shape and the volume fraction, inclusion morphology and distribution are characterized using quantitative metallography.

INTRODUCTION

A wide range of engineering materials often exhibits both anisotropic plastic behaviour and anisotropic failure properties. Plain carbon steels may contain large inclusions preferentially elongated in the rolling direction. Inclusion shape is commonly expected to be at the origin of anisotropic ductility (Mudry [8], Lautridou and Pineau [7]). Recently, Gologanu et al. [4, 6] have developed a micromechanistically–based model including void shape effect (GLD–model). Anisotropic plastic behaviour coupled with damage has also been analysed in a previous work Benzerga et al. [2].
The aim of this article is to model ductile fracture anisotropy using local approach concepts. The analysis is based on the improved version of the GLD model [6] implemented in the finite element code ZéBuLoN7 [3]. The model emphasizes the role of anisotropic void growth on ductile rupture. Description of final failure is done using a localization–based coalescence criterion (Perrin [9]). The model is applied to a hot–rolled ferritic–pearlitic steel containing elongated MnS inclusions.

EXPERIMENTS

Material characterisation

The investigated material is a ferritic–pearlitic steel of grade X52 cut from a rolled sheet (C = 0.17, S = 0.009, Mn = 1.23, Nb = 0.0038wt%). Tensile and compression tests were carried out on smooth specimens to identify the orthotropic behaviour of the material (Tab.1). A detailed analysis of inclusion distribution was performed on polished sections

*Ecole des Mines de Paris, Centre des Materiaux, UMR CNRS 7633 BP87 91003 Evry, France
†Gaz de France, BP 33, 93211 La Plaine St Denis Cedex, France

Table 1: Yield stress (σ_y), ultimate tensile strength (R_m), reduction of area ($Z\%$), anisotropy factor (R_ε) and strains to failure (ε_f) in notched bars AER for several notch radii. XY-axis : at 45° to X–axis in X-Y plane.

Tensile axis	σ_y (MPa)	R_m (MPa)	Z (%)	R_ε	ε_f (AER) (%)		
					10	4	2
L	405	532	120	$\varepsilon_S/\varepsilon_T = 1.5$	88.5	67.5	52.8
T	370	540	96	$\varepsilon_S/\varepsilon_L = 1.4$	55.7	36.9	26.0
LT	420	525	128	$\varepsilon_S/\varepsilon_{TL} = 1.1$	89.0	58.5	45.5

perpendicular to the orientations L, T and S. Only MnS, oxides or carbides greater than 2μm were considered. The mean dimensions $<d_i>$ of the inclusions in each section and their area fraction f_a were measured (Tab.2). Using stereological relationships, one can derive 3D average dimensions D_i of all inclusions [7]. In this study however, since we are mainly interested with MnS, we make use of the relationship $D_T=\sqrt{D_L D_S}$ (Batisse et al. [1]). Average dimensions D_i of MnS are reported in Tab.2. The volume fraction inferred from these calculations, equal to 0.09%, is comparable to f_a and to the value deduced from the chemical composition (Franklin formula): 0.045%.

Testing of notched bars

Tests on axisymmetric notched bars cut in L, T and LT orientations were carried out in order to study ductility anisotropy within a representative range of stress states. The specimen geometries noted AER are homothetic of standard ones (see e.g. [10]). Each test was interrupted several times to measure reduction of both principal diameters Φ_1 and Φ_2 and thus to estimate the average strain $\varepsilon = \ln(\Phi_0^2/(\Phi_1\Phi_2))$ where $\Phi_0 = 3.9$mm is the initial diameter. For any direction, the ductility decreases with increasing stress triaxiality (i.e. decreasing notch radius, see Tab.1). Note that the decrease in ductility in off–axis tension, LT, occurs more rapidly. It is worth noting the difference in the values of strains to failure between L and T directions.

MODELLING

Void Growth

The proposed model is developed in [4]-[6]. It consists in extending the Gurson criterion to the case of axisymmetric ellipsoidal cavities characterized by the shape parameter $S = \ln(a/b)$ (see Fig. 1). The latest version of the model [6] allows for a more realistic

Table 2: Quantitative metallography: mean dimensions and fraction of inclusions. ($\star$) refers to MnS only. (L) (resp. (T), (S)) is the section of normal L (resp. T, S).

$\mathcal{A}_a$ (μm^2/mm^2)			f_a	$<d_L>(\mu$m)		$<d_T>(\mu$m)		$<d_S>(\mu$m)		D_L	D_T	D_S
(L)	(T)	(S)	(%)	(T)	(S)	(L)	(S)	(L)	(T)	(μm)	(μm)	(μm)
364	1069	425	.06	14.6	4.4	3.8	3.2	3.1	2.6	–	–	–
				50.2*	11.2	–	2.9	–	2.	44.3	10.7	2.6

description of the evolution of void shape [11], with regards to unit cell calculations [13]. The model is formulated in terms of a yield criterion:

$$\Phi(\underset{\sim}{\Sigma}, f, S) = C\frac{||\underset{\sim}{\Sigma}' + \eta\Sigma_h\underset{\sim}{\mathbf{X}}||^2}{\sigma_\star^2} + 2q_w(g+1)(g+f)\cosh\left(\frac{\kappa\Sigma_h}{\sigma_\star}\right) - (g+1)^2 - q_w{}^2(g+f)^2 (1)$$

$$with \quad \Sigma_h = \alpha_2(\Sigma_{xx} + \Sigma_{yy}) + (1-2\alpha_2)\Sigma_{zz} \quad (2)$$

$\sigma_\star$ is the matrix flow stress, $\underset{\sim}{\Sigma}'$ the deviatoric part of $\underset{\sim}{\Sigma}$, $||\,||$ the von Mises norm, Σ_h a weighted average of the stresses, z–direction the common axis of the voids, $\underset{\sim}{\mathbf{X}}$ a constant tensor, and C, η, g, κ and α_2 are coefficients that depend only on the porosity f and S while α_1, ${\alpha_1}^G$ and q_w depend on S only. The evolution law of f is derived using mass conservation. The shape parameter evolution is governed by:

$$\dot{S} = \frac{3}{2}\left[1 + \frac{3}{2}h_{\mathcal{T}}(\mathcal{T})(1-\sqrt{f})^2\frac{\alpha_1 - {\alpha_1}^G}{1-3\alpha_1}\right]D'_{zz} + 3\left(\frac{1-3\alpha_1}{f} + 3\alpha_2 - 1\right)D_m \quad (3)$$

where D_m and D'_{zz} are the mean part of $\underset{\sim}{\mathbf{D}}$ and the $\underset{\sim}{\mathbf{D}}'$-component parallel to voids. See [6] for full expressions of S–functions and $h_{\mathcal{T}}(\mathcal{T})$, where $\mathcal{T}$ is the stress triaxiality. It is worth emphasizing that void growth is governed by Σ_h (which becomes the mean lateral stress in the cylindrical case, $\alpha_2 = 1/2$). Recently, a Gurson–like model incorporating plastic anisotropy effects has been proposed in the case of spherical voids [2]. No micromechanically-based model is still available accounting for both plastic anisotropy and void shape. Here, for simplicity's sake, we just replaced Mises equivalent stress by Hill equivalent stress in Eq.(1).

Coalescence

Final rupture is governed by void coalescence. In this work, coalescence is assumed to correspond to the development of highly porous layers in the material. The onset of coalescence occurs when the condition of strain localization is satisfied in a horizontal plane within the porous region [9]. Such a localization implies a vanishing hardening rate of the porous material (Rice [12]). Of course an accurate analysis of the coalescence mechanisms should incorporate void shape effects (Thomason [14], Gologanu et al. [5]). But the basic idea for coalescence modelling remains the inhomogeneous distribution of voids induced by the deformation.

RESULTS AND DISCUSSION

Void shape effect

The main drawback of the earliest model [4] is that the effect of S on the porosity rate was uncorrect [13]. If one explicitely calculates $\dot{f}$ from the criterion using the incompressibility condition and the normality flow rule then we obtain after some manipulations for axisymmetric stress states and $|S| > 1$:

$$\frac{\dot{f}}{1-f} = \frac{\frac{\partial_{\Sigma_h}\Phi}{\partial_{\Sigma_{eq}}\Phi}}{1-\beta\frac{\partial_{\Sigma_h}\Phi}{\partial_{\Sigma_{eq}}\Phi}}D_{eq}{}^{(p)} \quad \text{where} \quad \beta = \frac{1}{3}\text{, (prolate)}\,;\, -\frac{2}{3}\text{, (oblate)}\,;\, 0\text{, sphere} \quad (4)$$

It is the presence of Σ_h in the squared term of Φ in Eq. (1), that leads to a correct influence of the shape of the void upon its growth rate as shown by Eq. (4). For high triaxialities and $f \to 0$, one can also derive a cavity growth rate similar to that of Rice and Tracey but including the effect of shape change:

$$\frac{\dot{f}}{f} = \left(\frac{\frac{1}{2} q_w \kappa}{(1-\beta\eta)(\eta \mathcal{T}_h + 1) - \beta q_w \kappa f \sinh(\kappa \mathcal{T}_h)} \right) \exp(\kappa \mathcal{T}_h) \, D_{eq}{}^{(p)} \quad \text{where } \mathcal{T}_h - \frac{\Sigma_h}{\Sigma_{eq}} \quad (5)$$

Of course the shape parameter itself varies in the general case according to Eq. (3). Fig.-1 shows the evolution of S for different stress states, initial shapes and loading directions. These results are obtained through FE integration of the constitutive equations with stress state control using Riks algorithm. The fact that voids tend to become spherical at high triaxialities has received wide acceptance. This is obvious from Fig.-1 for initially prolate or oblate cavities. However, an initially spherical cavity tends to become oblate at high triaxiality ($\mathcal{T} \geq 2$ in Fig.-1). This is a typically plastic effect in qualitative agreement with the results of Budiansky et al. [15]. More generally, for a given S_0 there is an intermediate stress state $\mathcal{T}_i$ that let the void shape invariant during deformation (for instance, $\mathcal{T}_i(S_0 = 2.5) \approx 1$ while for spheres $\mathcal{T}_i(S_0 = 0) \approx 1.5$). Simulations done for loading perpendicularly to the void axis (dotted lines in Fig.- 1) generalize those presented in [5]. It is clear that S evolution is less sensitive to $\mathcal{T}$ than in the condition of loading parallel to voids. But at a given triaxiality $\mathcal{T}$, the evolution of shape parameter depends sufficiently on the loading direction to allow for strongly different effects on cavity growth according to Eq.(4). This will be of a great importance in the following when anisotropic rupture is considered. Finally, off–axis tension using the present model gives as expected poor results, since the model is valid only for parallel voids that do not rotate relative to the material.

Simulation of notched tensile bars

Fully-3D simulation of AER accounting for plastic anisotropy is done using ZéBuLoN code [3]. Quadratic quadrilaterals subintegrated elements with updated Lagrangian formulation are used. Calculations are mesh–insensitive as far as fracture initiation is considered. The element size is $0.5 \times 0.5 \times 0.25$ mm^3 at the minimal section of notched specimens. Yielding obeys Hill's criterion while the isotropic hardening law is fitted for L–direction [2]. Finally, use is made of the localization model to assess the critical porosities at coalescence. The set of equations established in the case of a Gurson–like metal [9] has been solved using MAPLE code for a wide range of triaxialities and f_0. Results obtained with the prolate model are shown in Fig.-2 with the initial mean values: $f_0 = .09\%$ and $S_0 = D_L/\sqrt{D_T D_S} = 1.5$. S_0 is lower than the value obtained for MnS only. The model correctly accounts for anisotropy effect since ductility is higher in L direction whatever the triaxiality. No attempt has been made to quantitatively improve these results by varying f_0. It is nevertheless likely that discrepancies between experimental and numerical results are due to the void shape effect on the coalescence process. The porosity is always maximum at the center of the minimal section whereas S distribution depends on S_0 and specimen geometry. For instance, for $AER4$ specimens (Fig.-3 and -4), S tends to decrease at the center, more rapidly in tension along T direction (Fig.-4) in agreement with experimental observations.

CONCLUSION AND FUTURE WORK

(1) The proposed model is formulated in terms of a macroscopic yield function depending on two appropriate variables physically meaningful and measurable.
(2) At high $\mathcal{T}$, voids do not necessarily tend to become spherical. That is why a simplified cavity growth law (Eq.(5)) is proposed to account for likely S-effect.
(3) A material with prolate cavities parallel to loading direction exhibits much higher ductility than a material containing spherical voids.
(4) Modelling anisotropic ductile rupture needs the use of at least two variables (f and S). It is thus possible to study separately the effects of S on cavity growth and void coalescence.
(5) Finally the three following topics have to be pursued: the need for a second shape parameter to model the short-transverse rupture; the treatment of the problem encountered in off-axis tension by incorporating cavity rotation; implications of the model with strain localization should be investigated further.

Acknowledgements: One of the authors (A.A. Benzerga) is sincerely grateful to Francis Curie from GDF for helpful contribution to the quantitative metallography.

REFERENCES

[1] R. Batisse, M. Bethmont, G. Devesa, and G. Rousselier. *Nuc. Eng. D.*, 105:113–120, 1988.

[2] A. Benzerga, J. Besson, and A. Pineau. J. P. B. Peseux et al. eds., 3^{eme} *Col. Nat. Cal. Struc.*, pp. 673–678. Pres. Acad. de l'Ouest, 20–23 Mai 1997.

[3] J. Besson and R. Foerch. *Comp. Meth. Appl. Mech. Eng.*, 142:165–187, 1997.

[4] M. Gologanu, J. Leblond, and J. Devaux. *J. Mech. Phys. Sol.*, 41(11):1723–54, 1993.

[5] M. Gologanu, J. Leblond, and J. Devaux. A. Needleman ed., *Computatinal Material Modeling*, pp 223–244, ASME, 1994.

[6] M. Gologanu, J. Leblond, and G. Perrin. *Cont. Micromechanics.*, P. Suquet ed., 1995.

[7] J. Lautridou and A. Pineau. *Eng. Frac. Mech*, 15(1-2):55–71, 1981.

[8] F. Mudry. PhD thesis, Doctorat d'état, Univ. Tech. Compiègne, 1982.

[9] G. Perrin. PhD thesis, Ecole Polytechnique, 1992.

[10] A. Pineau. Francois. et al. ed., *Adv. in Frac. Res.*, pp. 553–577. Pergamon, 1981.

[11] P. Ponte Castaneda and M. Zaidman. *J. Mechs. Phys. Solids*, 42:1459–1495, 1994.

[12] J. Rice. The localization of plastic deformation. W. Koiter ed., *14th int. cong. Theo. Appl. Mech*, pp. 207–220. North–Holland, 1976.

[13] O.P. Sovik. and C. Thaulow. *Fat. Fract. Engng. Mater. Struct.*, 20:1731–1744, 1997.

[14] P. F. Thomason. *Acta Metallurgica*, 33(6):1079–1085, 1985.

[15] B. Budiansky, J. W. Hutchinson, and S. Slutsky. M. J. Hopkins ed., *Mechanics of Solids, The R. Hill 60th Anniv. Vol.*, pp 13–45, 1982.

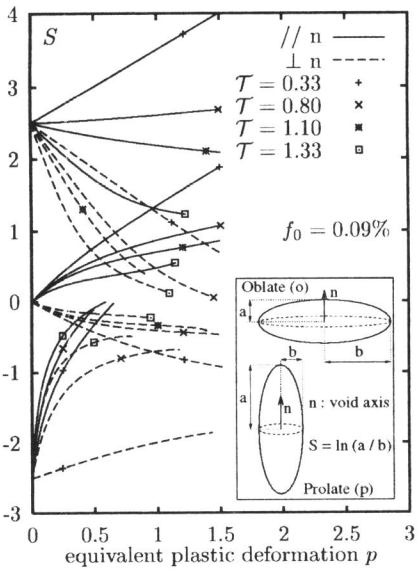

Figure 1: Definition and evolution of S for different $\mathcal{T}$, S_0 and loading directions.

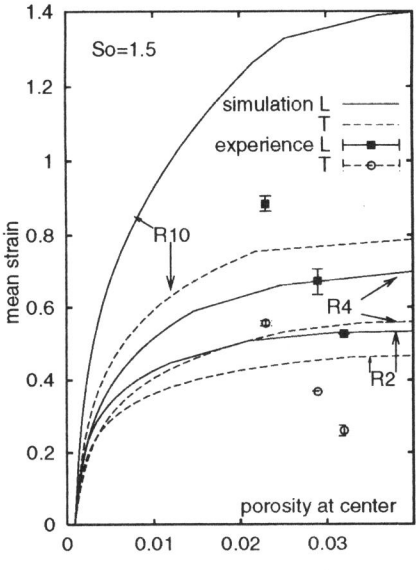

Figure 2: f–$\overline{\varepsilon}$ curves. Experimental values ε_f are given at values of f at coalescence.

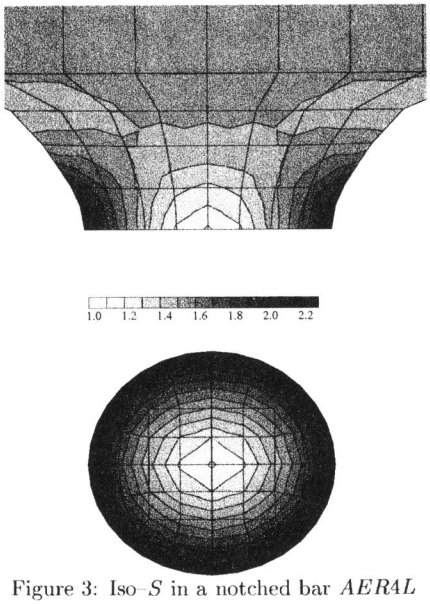

Figure 3: Iso–S in a notched bar *AER4L* (radius 4, tension along L) at coalescence.

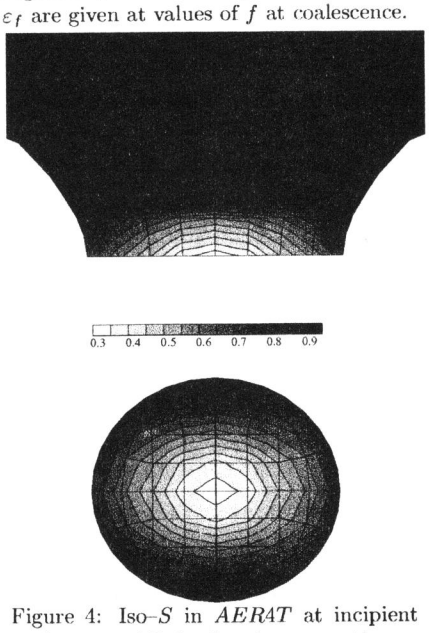

Figure 4: Iso–S in *AER4T* at incipient coalescence. Minimal and cross sections.